

# PCCP

Accepted Manuscript



This is an *Accepted Manuscript*, which has been through the Royal Society of Chemistry peer review process and has been accepted for publication.

*Accepted Manuscripts* are published online shortly after acceptance, before technical editing, formatting and proof reading. Using this free service, authors can make their results available to the community, in citable form, before we publish the edited article. We will replace this *Accepted Manuscript* with the edited and formatted *Advance Article* as soon as it is available.

You can find more information about *Accepted Manuscripts* in the [Information for Authors](#).

Please note that technical editing may introduce minor changes to the text and/or graphics, which may alter content. The journal's standard [Terms & Conditions](#) and the [Ethical guidelines](#) still apply. In no event shall the Royal Society of Chemistry be held responsible for any errors or omissions in this *Accepted Manuscript* or any consequences arising from the use of any information it contains.

## Noble Gas Encapsulation: Clathrate Hydrates and their HF Doped Analogues

Sukanta Mondal and Pratim Kumar Chattaraj\*

*Department of Chemistry and Center for Theoretical Studies, Indian Institute of Technology,  
Kharagpur, 721302, India.*

*\*To whom correspondence should be addressed. E-mail: [pkc@chem.iitkgp.ernet.in](mailto:pkc@chem.iitkgp.ernet.in),  
Telephone: +91-3222-283304, Fax: +91-3222-255303.*

### Abstract

Significance of clathrate hydrates lies in their ability to encapsulate a vast range of inert gases. Although the natural abundance of a few noble gases (Kr, Xe) is poor their hydrates are generally abundant. It has already been reported that HF doping enhances the stability of hydrogen hydrates and methane hydrates which prompted us to perform a model study on helium, neon and argon hydrates with their HF doped analogues. For this purpose  $5^{12}$ ,  $5^{12}6^8$  and their HF doped analogues are taken as the model clathrate hydrates which are among the building blocks of sI, sII and sH etc. types of clathrate hydrate crystals. We use the dispersion corrected and gradient corrected hybrid density functional theory for the calculation of thermodynamic parameters as well as conceptual density functional theory based reactivity descriptors. The method of the *ab initio* molecular dynamics (AIMD) simulation is used through atom centered density matrix propagation (ADMP) techniques to envisage the structural behaviour of different noble gas hydrates in a 500 fs time scale. Electron density analysis is carried out to understand the nature of Ng-OH<sub>2</sub>, Ng-FH and Ng-Ng interactions. Current results noticeably demonstrate that noble gas (He, Ne, Ar) encapsulation ability of  $5^{12}$ ,  $5^{12}6^8$  and their HF doped analogues is thermodynamically favourable.

## Introduction

Noble gases are unique owing to their chemical stability. Only in extreme physicochemical conditions these noble gases can be made to react to produce compounds. Among all the noble gases argon was discovered first. Lord Rayleigh and Sir William Ramsay discovered Argon in 1894 [1]. After a couple of years Villard introduced the argon hydrates [2], and discovery of argon hydrates was the first among the noble gas hydrates. Thus noble gas hydrates have emerged since the last decade of 19<sup>th</sup> century. Then in consecutive 3 decades hardly any work was done on noble gas hydrates and 1923 onwards de Forcrand started working on noble gas hydrates especially krypton and xenon hydrates [3, 4]. In the present work we would discuss mainly Helium, Neon and Argon hydrates.

London et al. showed that applying He gas pressures of  $> 0.28$  GPa, it is possible to achieve He-clathrate hydrates. He enclathration stabilizes the ice II structural framework whereas destabilizes the formation of ice III, V and IX [5]. Belosludov et al. made it known that He hydrate forms Ic ice structure where the stability of Ic structure increased substantially, when the cage is completely filled with He atoms and they concluded that helium hydrate He.H<sub>2</sub>O in ice Ic is more stable than ice VIII in the pressure range 4.24 to 5 kbar [6]. It is reported that ice I<sub>h</sub> can encapsulate one He atom, which is in a ratio of  $< 1:8$  with encapsulated D<sub>2</sub>O molecules at approximately 3 kbar pressure [7]. The formation of classical clathrate hydrates in aqueous neon, hydrogen, argon, krypton and xenon systems was reported by Dyadin et al., and they mentioned that as the size of the guest noble gas atoms increases their formation requires more pressure. They added that hydrogen and neon can form classical clathrate hydrate structure up to 15 kbar. Ar and Kr form hydrates based on the ice II framework at high pressure [8]. Hakim et al. studied the neon hydrate of ice Ic through isobaric grand-canonical Monte Carlo simulation [9]; they reported that, ice I<sub>c</sub> alone is less stable than that of the neon I<sub>c</sub> hydrate, and neon I<sub>c</sub> hydrate is more favourable than the neon hydrate of the ice II structure which was reported previously through experiment. It was also reported that ice II can encapsulate neon [10]. At pressure  $> 9.6$  kbar, Ar may form hydrate of ice structure VI [11]. Abbondandola and Anderson et al. in different studies delineated the formation of sII hydrates by Ar and propane guests [12-14]. In another study Abbondandola et al. discussed that propane hydrate can absorb more Ar respect to hydrogen but the absorption kinetics of Ar is slower than that of hydrogen by an order of two

[13]. All these studies revealed the need for further research on noble gas hydrates. Till now it is discovered that Ar can form sII hydrate with propane guest, but excluding that no one has reported the formation of sI or sII or sH hydrates by aforementioned noble gasses (He, Ne and Ar). Clathrate hydrate cage structures of type sI and sII are identified and characterized long back in the early 1950s [15-17]. In 1998 Sloan et al. reported the third kind of water clathrate of hexagonal cubic structure (sH) [18]. After the detailed knowledge on these sI, sII and sH clathrate hydrates, numerous articles were published on sI, sII and sH - hydrogen hydrates, methane hydrates, binary hydrates but hardly any result is reported on noble gas (He, Ne and Ar) hydrates of these crystal structures. Low stability of noble gas hydrates may be the strong reason behind this.

Following our previous calculations on hydrogen hydrates, HF-doped hydrogen hydrates and methane hydrates [19-22] here we have checked the stability of noble gas hydrates and compared their stability and dynamics with HF doped noble gas hydrates. The character of interaction among noble gas atoms and water cage wall as well as the interaction among encapsulated noble gas atoms are studied through the assessment of electron density and electron density based descriptors. Stability and dynamics of the noble gas encapsulated hydrates and their HF doped analogues at different temperatures are investigated in course of time using *ab initio* molecular dynamics [23] simulations through an Atom Centered Density Matrix Propagation (ADMP) [24-26] technique.

## Theory and computation

Hardness ( $\eta$ ) and electrophilicity ( $\omega$ ) in conjunction with the associated electronic structure principles like the maximum hardness principle [27-30] (MHP) and minimum electrophilicity principle [30, 31] (MEP) are the parameters which we use to assess the stability of molecular systems, The electronegativity [32, 33] ( $\chi$ ), hardness [34, 35] ( $\eta$ ) and electrophilicity ( $\omega$ ) [36] of an N-electron system can be defined as follows:

$$\chi = -\mu = -\left(\frac{\partial E}{\partial N}\right)_{v(\bar{r})} \quad (1)$$

$$\eta = \left( \frac{\partial^2 E}{\partial N^2} \right)_{v(\vec{r})} \quad (2)$$

$$\omega = \frac{\mu^2}{2\eta} = \frac{\chi^2}{2\eta} \quad (3)$$

Here  $E$ ,  $\mu$  and  $v(\vec{r})$  are the total energy of the  $N$ -electron system, chemical potential and external potential, respectively.

Applying finite difference approximation, Eqs.1 and 2 can be expressed as:

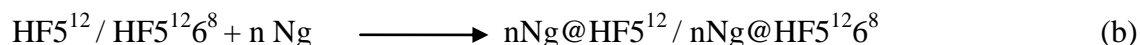
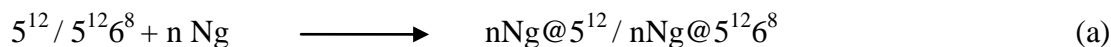
$$\chi = \frac{I + A}{2} \quad (4)$$

$$\text{and} \quad \eta = I - A \quad (5)$$

where  $I$  and  $A$  are the ionization potential and electron affinity of the molecular system, respectively.  $I$  and  $A$  are calculated, using the energies of the corresponding frontier molecular orbitals through Koopmans' theorem [37]. It is known that the validity of Koopmans' theorem is within the Hartree-Fock theory but one can use the same approach with the help of Janak's theorem [38] in Kohn-Sham computations.

Graphical software, GaussView 5 [39] is used for the modelling and analysis of different input and output geometries. All the optimizations, frequency calculations and molecular dynamics simulations are done using Gaussian 09 package [40]. Geometry optimization of all the modelled structures is done using the  $\omega$ B97X-D [41] functional containing empirical dispersion in conjunction with 6-311+G(d,p) basis set.

Working equations (7) and (8) are employed to calculate the binding energy (as well as interaction enthalpy) for the encapsulation of noble gasses by using the scheme (a) and (b) respectively,



$$\Delta E = (1/n)[E_{N_g@Clathrate} - (E_{Clathrate} + nE_{N_g})] \quad (7)$$

$$\Delta E = (1/n)[E_{N_g@HFClathrate} - (E_{HFClathrate} + nE_{N_g})] \quad (8)$$

in equation (7),  $\Delta E$ ,  $E_{N_g@Clathrate}$ ,  $E_{Clathrate}$  and  $E_{N_g}$  denote the binding energy (or interaction energy) of noble gas encapsulation, energy of noble gas encapsulated clathrate hydrate, energy of clathrate hydrate and energy of noble gas atom respectively. In equation (8)  $\Delta E$ ,  $E_{N_g@HFClathrate}$ ,  $E_{HFClathrate}$  denote the binding energy of noble gas encapsulation by HF doped clathrate hydrate, energy of noble gas encapsulated HF doped clathrate hydrate and energy of HF doped clathrate hydrate respectively. Energies of noble gas encapsulated clathrate hydrates are computed using the basis set superposition error (BSSE) correction as well by the standard counterpoise (CP) method of Boys and Bernardi [42]. Dynamics of the maximum noble gas atom encapsulated clathrate hydrates and their HF doped analogues are studied through *ab initio* molecular dynamics simulation [23], using Atom Centered Density Matrix Propagation (ADMP) [24-26] technique included in the Gaussian 09 program package. The simulations are performed at B3LYP/6-31G(d) [43-44] level of theory with initial geometries corresponding to minimum energies (calculated at  $\omega$ B97X-D/6-311+G(d,p) level) of different systems. Simulation is done at different temperatures to see the dynamical behaviour of the noble gas clusters inside the water cage as well as the structural change (if any) of the clathrate hydrate and their HF doped analogues. Initial nuclear kinetic energies of the systems are generated by using a Boltzmann distribution. Velocity scaling thermostat is used to maintain the temperature throughout the simulation. We used default random number generator seed, implemented in G09 to initiate the initial mass weighted Cartesian velocity. In all the cases simulation is done by keeping the fictitious electronic mass as 0.1 amu.

## Results and discussion

For the assessment of noble gas (He, Ne, Ar) encapsulation ability of clathrate hydrates and their HF doped analogues we have taken two representative hydrate cages: one small ( $5^{12}$ ) and one big ( $5^{12}6^8$ ) (Figure S1) (see Supplementary Information). The notation  $5^{12}$  indicates a cage with 12 pentagonal faces and the notation  $5^{12}6^8$  stands for a cage with 12 pentagonal and 8 hexagonal faces. These two unit cages are among the basic building blocks of different clathrate hydrate

crystals, namely sI, sII and sH etc. These two cages and their HF doped analogues are modelled according to the structures previously reported by us [21, 22]. All the noble gas encapsulated clathrate hydrates are modelled without destroying the structural integrity and shape, and only those optimized geometries are considered for further study where structural integrity and overall shape remains intact. Though in a few cases symmetric changes in shape are observed and they are considered for further study. Absence of any imaginary frequency in the calculated harmonic vibrational frequencies of the optimized structures confirms that the optimized noble gas clathrate hydrate structures correspond to minima on the potential energy surface. All the energy minima structures are given in Figure S2. Interaction energy and BSSE corrected interaction energy for the encapsulation of each noble gas atom is calculated following the equations (7) and (8).

$5^{12}$  and  $\text{HF}5^{12}$  (HF doped  $5^{12}$  cage) can trap up to five helium atoms, three neon atoms and two argon atoms. It is observed that five helium atoms form a trigonal-bipyramid cluster inside the  $5^{12}$  and  $\text{HF}5^{12}$  cages. In  $4\text{He}@5^{12}$  /  $4\text{He}@\text{HF}5^{12}$ , helium atoms form trigonal-pyramidal arrangement whereas in  $3\text{He}@5^{12}$  /  $3\text{He}@\text{HF}5^{12}$  helium atoms stay in a trigonal arrangement. But the interaction energy ( $\Delta E$ , kcal/mol), BSSE corrected interaction energy ( $\Delta E_{\text{BSSE}}$ , kcal/mol) and interaction enthalpy ( $\Delta H$ , kcal/mol) values (Table 1) reveal that only the encapsulation of the first helium atom is energetically favourable; though the  $\Delta E$ ,  $\Delta E_{\text{BSSE}}$  and  $\Delta H$  values for the encapsulation of second and third helium atoms are slightly positive. It is clear that the  $\Delta E$ ,  $\Delta E_{\text{BSSE}}$  and  $\Delta H$  values differ very little in  $5^{12}$  and  $\text{HF}5^{12}$  systems. The arrangement of three neon atoms inside the water cage is trigonal-planar. The interaction energy, BSSE corrected interaction energy and interaction enthalpy for the encapsulation of the first neon atom reveal that the encapsulation may be a favourable process but for the second and the third neon atoms both become positive. The  $\Delta E$  and  $\Delta H$  values in the case of the HF doped cage are slightly more negative than that of the undoped one.  $5^{12}$  and  $\text{HF}5^{12}$  can trap two argon atoms where the encapsulation of the first one is energetically favourable, the interaction energy, BSSE corrected interaction energy and interaction enthalpy are negative but the encapsulation of the second argon atom is not favourable as the  $\Delta E$ ,  $\Delta E_{\text{BSSE}}$  and  $\Delta H$  are positive. For the encapsulation of the first argon atom it is observed that the interaction energy, BSSE corrected interaction energy and interaction enthalpy values are more negative in the case of HF doped clathrate hydrate. Both the

cages of  $2\text{Ar}@5^{12}$  and  $2\text{Ar}@HF5^{12}$  become egg shaped from a spherical one which reveals that the cavity size of  $5^{12}$  and  $HF5^{12}$  cages are not enough to hold two argon atoms though we obtained minima on the potential energy surface.

**Table 1.** Interaction energy ( $\Delta E$ , kcal/mol), BSSE corrected interaction energy ( $\Delta E_{BSSE}$ , kcal/mol) and interaction enthalpy ( $\Delta H$ , kcal/mol) per Ng atom for the reaction,  $5^{12} / HF5^{12} + n\text{Ng}$  ( $n=1-6$ )  $\longrightarrow$   $n\text{Ng}@5^{12} / n\text{Ng}@HF5^{12}$  for  $n$  Ng ( $n=1-5$  (He),  $1-3$  (Ne),  $1-2$  (Ar)) Encapsulation.

Systems	$\Delta E$	$\Delta E_{BSSE}$	$\Delta H$	Systems	$\Delta E$	$\Delta E_{BSSE}$	$\Delta H$
$1\text{He}@5^{12}$	-0.90	-0.62	-0.56	$1\text{He}@HF5^{12}$	-0.90	-0.62	-0.58
$2\text{He}@5^{12}$	0.23	0.52	0.64	$2\text{He}@HF5^{12}$	0.12	0.41	0.60
$3\text{He}@5^{12}$	0.49	0.77	0.91	$3\text{He}@HF5^{12}$	0.50	0.79	0.96
$4\text{He}@5^{12}$	1.04	1.32	1.56	$4\text{He}@HF5^{12}$	1.10	1.38	1.61
$5\text{He}@5^{12}$	1.78	2.03	2.33	$5\text{He}@HF5^{12}$	1.77	2.03	2.35
$1\text{Ne}@5^{12}$	-2.63	-1.61	-2.19	$1\text{Ne}@HF5^{12}$	-2.65	-1.61	-2.28
$2\text{Ne}@5^{12}$	0.13	1.23	0.76	$2\text{Ne}@HF5^{12}$	-0.10	1.01	0.51
$3\text{Ne}@5^{12}$	1.13	2.23	1.70	$3\text{Ne}@HF5^{12}$	1.17	2.29	1.74
$1\text{Ar}@5^{12}$	-3.26	-2.59	-2.83	$1\text{Ar}@HF5^{12}$	-3.80	-3.13	-3.35
$2\text{Ar}@5^{12}$	5.14	5.90	5.66	$2\text{Ar}@HF5^{12}$	5.44	6.21	6.22

The average diameter of the  $5^{12}$  and  $5^{12}6^8$  cages are 7.86 Å and 11.42 Å respectively.  $5^{12}$  cage contains 20 vertices whereas  $5^{12}6^8$  cage contains 36 vertices [45]. Cavity size of the  $5^{12}6^8$  cage is much greater than that of the  $5^{12}$  cage.

$5^{12}6^8$  cage can encapsulate 9 He atoms whereas  $HF5^{12}6^8$  (HF doped  $5^{12}6^8$  cage) cage can encapsulate 10 He atoms. All the trials we made to optimize the 10He encapsulated  $5^{12}6^8$  cage ended with a distorted, ruptured cage or we have not found minima on the potential energy surface and we excluded the 10 He encapsulated  $5^{12}6^8$  cage from our study. We observed minima on the potential energy surface for the entire set of reported He encapsulated  $5^{12}6^8$  systems and  $HF5^{12}6^8$  systems. Encapsulated helium atoms inside the cage form a helium cluster.

He clusters inside  $5^{12}6^8$  and in  $HF5^{12}6^8$  cages are more or less of similar geometric shapes (Table 2).

**Table 2.** Geometric shapes of the encapsulated He clusters in  $5^{12}6^8$  and  $HF5^{12}6^8$  clathrate hydrates.

Systems	Arrangement of He cluster	Systems	Arrangement of He cluster
$3\text{He}@5^{12}6^8$	Tringular	$3\text{He}@HF5^{12}6^8$	Tringular
$4\text{He}@5^{12}6^8$	Non planner tetragonal (two triangular planes joined through two He atoms)	$4\text{He}@HF5^{12}6^8$	Non planner tetragonal (two triangular planes joined through two He atoms)
$5\text{He}@5^{12}6^8$	Distorted trigonal bipyramidal	$5\text{He}@HF5^{12}6^8$	Distorted trigonal bipyramidal
$6\text{He}@5^{12}6^8$	Square bipyramidal	$6\text{He}@HF5^{12}6^8$	Square bipyramidal
$7\text{He}@5^{12}6^8$	Pentagonal bi pyramidal	$7\text{He}@HF5^{12}6^8$	Pentagonal bi pyramidal
$8\text{He}@5^{12}6^8$	Hexagonal bipyramidal	$8\text{He}@HF5^{12}6^8$	Hexagonal bipyramidal
$9\text{He}@5^{12}6^8$	Distorted hexagonal bipyramidal and one He atom holds the centre of the hexagonal plane	$9\text{He}@HF5^{12}6^8$	Distorted hexagonal bipyramidal and one He atom holds the centre of the hexagonal plane
$10\text{He}@5^{12}6^8$	--	$10\text{He}@HF5^{12}6^8$	Dodecahedral

**Table 3.** Interaction energy ( $\Delta E$ , kcal/mol), BSSE corrected interaction energy ( $\Delta E_{BSSE}$ , kcal/mol) and interaction enthalpy ( $\Delta H$ , kcal/mol) per Ng atom for the reaction,  $5^{12}6^8 / HF5^{12}6^8 + n\text{Ng}$  ( $n=1-6$ )  $\longrightarrow$   $n\text{Ng}@5^{12}6^8 / n\text{Ng}@HF5^{12}6^8$  for  $n$  Ng ( $n=1-9/10$  (He),  $1-6$  (Ne, Ar)) encapsulation.

Systems	$\Delta E$	$\Delta E_{BSSE}$	$\Delta H$	Systems	$\Delta E$	$\Delta E_{BSSE}$	$\Delta H$
$1\text{He}@5^{12}6^8$	-0.54	-0.35	-0.21	$1\text{He}@HF5^{12}6^8$	-0.60	-0.39	-0.28
$2\text{He}@5^{12}6^8$	-0.60	-0.39	-0.26	$2\text{He}@HF5^{12}6^8$	-0.60	-0.39	-0.24
$3\text{He}@5^{12}6^8$	-0.57	-0.38	-0.23	$3\text{He}@HF5^{12}6^8$	-0.56	-0.37	-0.26
$4\text{He}@5^{12}6^8$	-0.58	-0.39	-0.25	$4\text{He}@HF5^{12}6^8$	-0.58	-0.39	-0.27
$5\text{He}@5^{12}6^8$	-0.58	-0.39	-0.25	$5\text{He}@HF5^{12}6^8$	-0.58	-0.39	-0.25
$6\text{He}@5^{12}6^8$	-0.55	-0.36	-0.22	$6\text{He}@HF5^{12}6^8$	-0.55	-0.36	-0.23
$7\text{He}@5^{12}6^8$	-0.38	-0.20	-0.05	$7\text{He}@HF5^{12}6^8$	-0.47	-0.28	-0.12
$8\text{He}@5^{12}6^8$	-0.20	-0.02	0.14	$8\text{He}@HF5^{12}6^8$	-0.20	-0.02	0.14

9He@5 <sup>12</sup> 6 <sup>8</sup>	-0.12	0.07	0.24	9He@HF5 <sup>12</sup> 6 <sup>8</sup>	-0.11	0.07	0.23
10He@5 <sup>12</sup> 6 <sup>8</sup>	-	-	-	10He@HF5 <sup>12</sup> 6 <sup>8</sup>	-0.17	0.01	0.18
1Ne@5 <sup>12</sup> 6 <sup>8</sup>	-1.34	-0.87	-1.02	1Ne@HF5 <sup>12</sup> 6 <sup>8</sup>	-1.52	-1.00	-1.08
2Ne@5 <sup>12</sup> 6 <sup>8</sup>	-1.53	-0.99	-1.12	2Ne@HF5 <sup>12</sup> 6 <sup>8</sup>	-1.54	-1.00	-1.17
3Ne@5 <sup>12</sup> 6 <sup>8</sup>	-1.59	-1.03	-1.20	3Ne@HF5 <sup>12</sup> 6 <sup>8</sup>	-1.57	-1.01	-1.40
4Ne@5 <sup>12</sup> 6 <sup>8</sup>	-1.65	-1.05	-1.25	4Ne@HF5 <sup>12</sup> 6 <sup>8</sup>	-1.67	-1.07	-1.29
5Ne@5 <sup>12</sup> 6 <sup>8</sup>	-1.49	-0.85	-1.08	5Ne@HF5 <sup>12</sup> 6 <sup>8</sup>	-1.72	-1.08	-1.31
6Ne@5 <sup>12</sup> 6 <sup>8</sup>	-1.61	-0.96	-1.21	6Ne@HF5 <sup>12</sup> 6 <sup>8</sup>	-1.61	-0.96	-1.23
1Ar@5 <sup>12</sup> 6 <sup>8</sup>	-2.17	-1.91	-1.81	1Ar@HF5 <sup>12</sup> 6 <sup>8</sup>	-2.47	-2.17	-2.13
2Ar@5 <sup>12</sup> 6 <sup>8</sup>	-2.03	-1.69	-1.67	2Ar@HF5 <sup>12</sup> 6 <sup>8</sup>	-2.58	-2.24	-2.23
3Ar@5 <sup>12</sup> 6 <sup>8</sup>	-2.05	-1.67	-1.68	3Ar@HF5 <sup>12</sup> 6 <sup>8</sup>	-2.09	-1.71	-1.75
4Ar@5 <sup>12</sup> 6 <sup>8</sup>	-1.43	-1.02	-1.08	4Ar@HF5 <sup>12</sup> 6 <sup>8</sup>	-1.60	-1.19	-1.29
5Ar@5 <sup>12</sup> 6 <sup>8</sup>	-1.28	-0.86	-0.98	5Ar@HF5 <sup>12</sup> 6 <sup>8</sup>	-1.24	-0.80	-0.82
6Ar@5 <sup>12</sup> 6 <sup>8</sup>	-0.46	-0.03	-0.03	6Ar@HF5 <sup>12</sup> 6 <sup>8</sup>	-0.44	0.00	0.05

The interaction energy and BSSE corrected interaction energy are negative for the encapsulation of up to eight helium atoms but the interaction enthalpy is negative for the encapsulation of up to 7 helium atoms (Table 3). Thus encapsulation of up to 7 helium atoms is thermodynamically favourable for 5<sup>12</sup>6<sup>8</sup> and HF5<sup>12</sup>6<sup>8</sup> cages. It is clear that the  $\Delta E$ ,  $\Delta E_{\text{BSSE}}$  and  $\Delta H$  values differ little in 5<sup>12</sup>6<sup>8</sup> and HF5<sup>12</sup>6<sup>8</sup> systems. Accordingly HF doping has very little effect on the interaction energy and interaction enthalpy for the encapsulation of helium atoms in 5<sup>12</sup>6<sup>8</sup> cage. In the cases of the neon and argon we get minima on the potential energy surface up to the six Ng (Ne and Ar) atoms encapsulated 5<sup>12</sup>6<sup>8</sup> and HF5<sup>12</sup>6<sup>8</sup> systems. It is observed that neon and argon both form clusters in the 5<sup>12</sup>6<sup>8</sup> and HF5<sup>12</sup>6<sup>8</sup> cages. In 6Ne@5<sup>12</sup>6<sup>8</sup> / 6Ne@HF5<sup>12</sup>6<sup>8</sup> and 6Ar@5<sup>12</sup>6<sup>8</sup> / 6Ar@HF5<sup>12</sup>6<sup>8</sup> neon and argon atoms stay in octahedral geometry. In 5Ne@5<sup>12</sup>6<sup>8</sup> / 5Ne@HF5<sup>12</sup>6<sup>8</sup> and 5Ar@5<sup>12</sup>6<sup>8</sup> / 5Ar@HF5<sup>12</sup>6<sup>8</sup> neon and argon atoms form trigonal bipyramidal or distorted trigonal bipyramidal clusters. Neon and argon atoms in 4Ne@5<sup>12</sup>6<sup>8</sup> / 4Ar@5<sup>12</sup>6<sup>8</sup> make non-planar tetragonal (two triangular planes joined through two Ng atoms) type of geometry whereas their HF doped analogues achieve trigonal pyramidal shapes. When the number of Ne / Ar atoms inside the water cage is three they form triangular clusters. The  $\Delta E$ ,  $\Delta E_{\text{BSSE}}$  and the  $\Delta H$  values (Table 3) for the encapsulation of neon and argon atoms are all negative (excluding the slightly

positive  $\Delta E_{\text{BSSE}}$  and  $\Delta H$  value for  $6\text{Ar}@HF5^{12}6^8$ ) indicating that the encapsulation of up to 6 neon and 5 argon atoms by the  $5^{12}6^8$  and  $HF5^{12}6^8$  cages are thermodynamically favourable. As the number of neon atom increases the  $\Delta E$  and  $\Delta H$  values become overall more negative whereas in the case of argon atom the reverse is true. Interaction energy and interaction enthalpy for the encapsulation of Ng is the highest for argon and the lowest for helium in the studied systems. One probable reason behind this is the size of the encapsulated guest molecule. The interaction energy, BSSE corrected interaction energy and interaction enthalpy for the encapsulation of Ng are greater for  $5^{12}$  than that in  $5^{12}6^8$ . Another important aspect is that the interaction energy and interaction enthalpy values are little more negative in the case of the HF doped clathrate hydrate. Thus the encapsulation of Ng atoms by clathrate hydrates is more favourable when the encapsulating cage is smaller in size (small cage radius), the radius of encapsulated Ng atom increases and their number decreases and when the cage is HF doped.

From the Table S1 it is clear that the hardness value increases and the electrophilicity value decreases steadily for the encapsulation of helium, neon and argon by  $5^{12}$  and  $HF5^{12}$  systems which corroborates well with the energy change and enthalpy change for the encapsulation of the first Ng atoms. Another important point to note that for the encapsulation of the first Ng atoms hardness value is higher in the case of HF doped cage in comparison to the undoped one which supports the fact that HF doped cage is more efficient in encapsulating noble gas (He, Ne, and Ar) atoms. For the encapsulation of the helium, neon and argon by the  $5^{12}6^8$  and  $HF5^{12}6^8$  cages it is observed (Table S2) that initially the hardness value decreases and the electrophilicity value increases (for the encapsulation of the first Ng atoms excluding He) after that hardness value increases and the electrophilicity value decreases. For all the cases the hardness (and electrophilicity) value of the HF doped system is higher (and lower) than that of the HF undoped analogues.

### **Nature of interaction: Electron density analysis**

The bond critical point (BCP) is calculated first using the Multiwfn program package [46]; then topological parameters are calculated at the obtained BCPs on Ng-O bonds, Ng-F bonds and on Ng-Ng bonds and are given in Table 4. Topological parameters, electron density ( $\rho(r_c)$ ), Laplacian of electron density ( $\nabla^2\rho(r_c)$ ), local kinetic energy density ( $G(r_c)$ ), local potential

energy density ( $V(r_c)$ ) and local electron energy density ( $H(r_c)$ ) are calculated (provided in Table 4) at the bond critical points to understand the nature of interaction in between Ng and oxygen of water cage (in Ng---O bond), in between Ng and fluorine of HF in HF doped cage (in Ng---F bond) and in between Ng atoms (Ng---Ng bonds). When the value of  $\nabla^2\rho(r_c)$  is negative it indicates the concentration of electron density (covalent interaction) whereas when the value of  $\nabla^2\rho(r_c)$  is positive it indicates the depletion of electron density (noncovalent interaction) [47]. In all the cases it is observed that the value of  $\nabla^2\rho(r_c)$  is small and positive whereas the value of  $\rho(r_c)$  is very small thus all the interactions given in table 4 are of noncovalent type. High and low values of  $\rho(r_c)$  indicate covalent and noncovalent interactions respectively. But we should not conclude only on the basis of  $\rho(r_c)$  and  $\nabla^2\rho(r_c)$  as they fail to describe the molecules  $F_2$  and CO [48, 49]. According to Cremer et al [50] if the values of  $\nabla^2\rho(r_c)$  is positive and  $H(r_c)$  is also positive then the interactions are noncovalent in nature. Table 4 shows that  $\nabla^2\rho(r_c)$  is positive and  $H(r_c)$  values are also all positive thus the studied interactions are purely noncovalent in nature. The negative value of the ratio of  $G(r_c)$  and  $V(r_c)$  indicates the existence of covalency in bonding [51]. As the value of  $-G(r_c)/V(r_c)$  is greater than 1 (Table 4) for all the BCPs in Ng---O, Ng---F, and Ng---Ng bonds the interactions are purely noncovalent in nature.

**Table 4.** Electron density descriptors (au) at the bond critical points of Ng and X (O/F/Ng) obtained from the wave functions generated at  $\omega$ B97X-D /6-311+g(d,p) level of theory.

System	Bond Critical Point	$\rho(r_c)$	$\nabla^2\rho(r_c)$	$G(r_c)$	$V(r_c)$	$H(r_c)$	$-G(r_c)/V(r_c)$
5He@5 <sup>12</sup>	He--●—O	0.0047	0.0252	0.0048	-0.0032	0.0016	1.5000
	He--●—He	0.0051	0.0311	0.0053	-0.0029	0.0024	1.8276
5He@HF5 <sup>12</sup>	He--●—O	0.0066	0.0307	0.0060	-0.0043	0.0017	1.3953
	He--●—F	0.0054	0.0292	0.0056	-0.0038	0.0018	1.4737
	He--●—He	0.0057	0.0352	0.0061	-0.0033	0.0028	1.8485
9He@5 <sup>12</sup> 6 <sup>8</sup>	He--●—O	0.0026	0.0119	0.0022	-0.0015	0.0007	1.4667
	He--●—He	0.0017	0.0092	0.0016	-0.0010	0.0006	1.6000
10He@HF5 <sup>12</sup> 6 <sup>8</sup>	He--●—O	0.0013	0.0072	0.0013	-0.0008	0.0005	1.6250
	He--●—F	0.0014	0.0078	0.0013	-0.0008	0.0005	1.6250
	He--●—He	0.0022	0.0118	0.0021	-0.0012	0.0009	1.7500
3Ne@5 <sup>12</sup>	Ne--●—O	0.0048	0.0240	0.0050	-0.0039	0.0011	1.2821
	Ne--●—Ne	0.0095	0.0548	0.0125	-0.0114	0.0011	1.0965

3Ne@HF5 <sup>12</sup>	Ne--●—O	0.0061	0.0302	0.0064	-0.0053	0.0011	1.2075
	Ne--●—F	0.0054	0.0286	0.0061	-0.0050	0.0011	1.2200
	Ne--●—Ne	0.0084	0.0501	0.0113	-0.0100	0.0013	1.1300
6Ne@5 <sup>12</sup> 6 <sup>8</sup>	Ne--●—O	0.0025	0.0139	0.0026	-0.0018	0.0008	1.4444
	Ne--●—Ne	0.0008	0.0080	0.0013	-0.0006	0.0007	2.1667
6Ne@HF5 <sup>12</sup> 6 <sup>8</sup>	Ne--●—O	0.0019	0.0108	0.0020	-0.0013	0.0007	1.5385
	Ne--●—F	0.0010	0.0074	0.0012	-0.0006	0.0006	2.0000
	Ne--●—Ne	0.0010	0.0092	0.0015	-0.0008	0.0007	1.8750
2Ar@5 <sup>12</sup>	Ar--●—O	0.0093	0.0414	0.0086	-0.0068	0.0018	1.2647
	Ar--●—Ar	0.0150	0.0700	0.0148	-0.0120	0.0028	1.2333
2Ar@HF5 <sup>12</sup>	Ar--●—O	0.0100	0.0394	0.0084	-0.0070	0.0014	1.2000
	Ar--●—F	0.0059	0.0254	0.0052	-0.0040	0.0012	1.3000
	Ar--●—Ar	0.0151	0.0705	0.0149	-0.0121	0.0028	1.2314
6Ar@5 <sup>12</sup> 6 <sup>8</sup>	Ar--●—O	0.0045	0.0170	0.0034	-0.0026	0.0008	1.3077
	Ar--●—Ar	0.0057	0.0253	0.0047	-0.0031	0.0016	1.5161
6Ar@HF5 <sup>12</sup> 6 <sup>8</sup>	Ar--●—O	0.0032	0.0151	0.0029	-0.0020	0.0009	1.4500
	Ar--●—F	0.0038	0.0175	0.0034	-0.0023	0.0011	1.4783
	Ar--●—Ar	0.0033	0.0139	0.0025	-0.0016	0.0009	1.5625

### **Ab initio Simulation**

It is observed that among 5<sup>12</sup>, 5<sup>12</sup>6<sup>8</sup> and their HF doped analogues, 5<sup>12</sup> and its HF doped analogue can encapsulate only one helium, one neon or one argon atom with negative interaction energy. We have done 500 fs simulation study on Ng@5<sup>12</sup> and Ng@HF5<sup>12</sup> systems at 298 K and observed that all the cages remain intact up to 500 fs and only little distortion is observed in the cage wall in the cases of Ne@5<sup>12</sup> and Ar@5<sup>12</sup> (Figure 1). Throughout the entire 500 fs simulation Ng atoms remain inside the cage (Figure 1), which reveals their kinetic stability at 298 K temperature. Thus we can say that the encapsulation of one helium, one neon or one argon atom by 5<sup>12</sup> and HF5<sup>12</sup> cages are thermodynamically as well as kinetically favourable (at 298 K). In the case of the He atom both the HF doped and undoped cages behave almost equally; only one structural feature is observed that HF doped cages are less distorted than the undoped cages during the 500 fs simulation study for the cases of neon and argon clathrate hydrates (Figure 1).

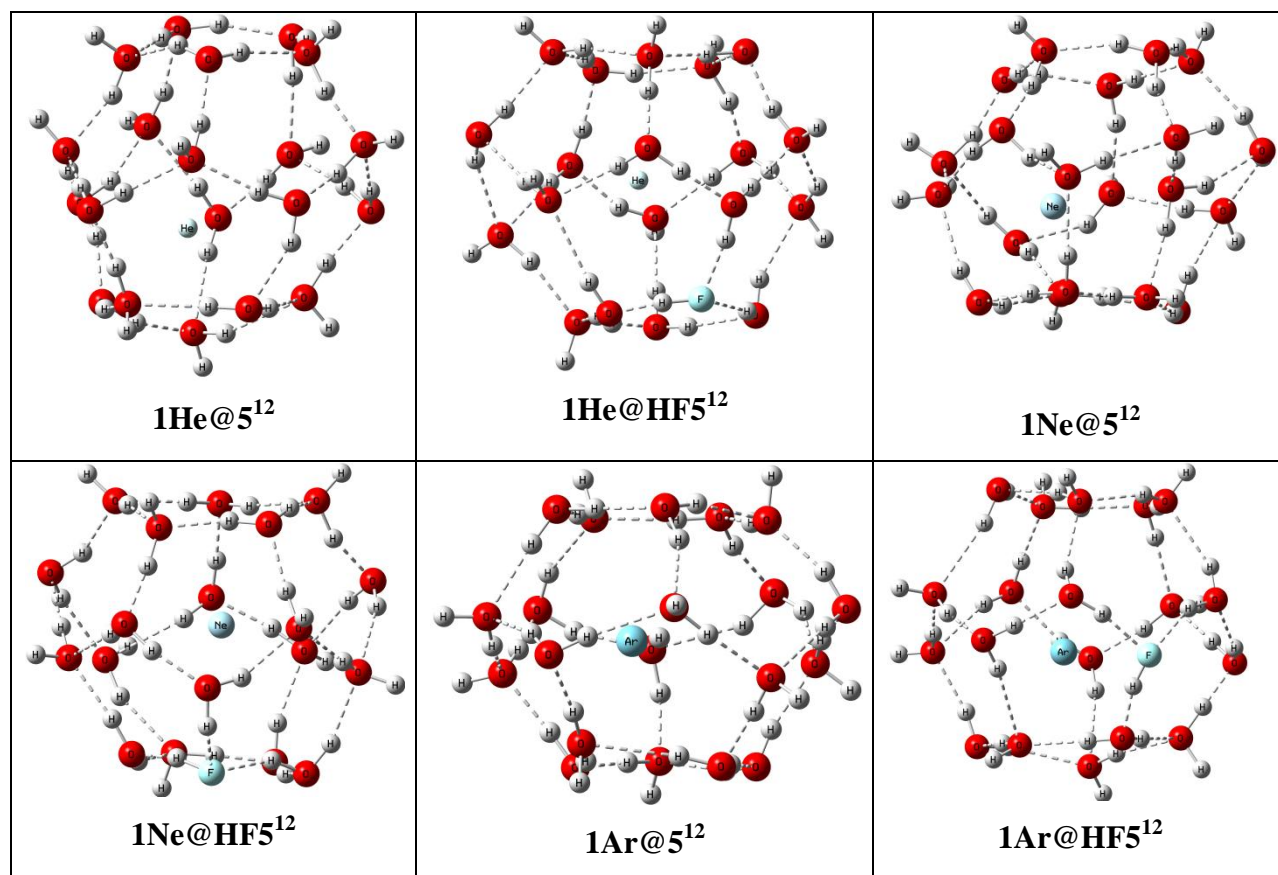


**Figure 1:** The structure of  $1Ng@5^{12}$  and  $1Ng@HF5^{12}$  systems ( $Ng = He, Ne$  and  $Ar$ ) at 298 K temperature at 500 fs.

In the cases of  $Ng@5^{12}6^8$  and  $Ng@HF5^{12}6^8$  systems the simulation study would not be simple like  $Ng@5^{12}$  and  $Ng@HF5^{12}$  systems as  $5^{12}6^8$  and  $HF5^{12}6^8$  cages can encapsulate up to nine or ten helium atoms, six neon atoms and six argon atoms. Here first of all we have done simulation at 298 K and have observed that most of the systems get distorted and ruptured thus we have done simulation up to 500 fs at 225 K, 175 K and 77 K temperatures as well. It is observed that irrespective of the temperature and the molecular system there is a maximum at 15 fs which may be due to the fact that the minimum energy molecular system takes 15 fs time to move out of the potential well.

### **$9He@5^{12}6^8$ & $10He@HF5^{12}6^8$ systems**

In the case of the  $9He@5^{12}6^8$  system, at 77 K and at 150 K simulations we observe that there is no structural change in the  $5^{12}6^8$  cage throughout the simulation. In the total energy profile we see broad maximum and minimum due to the distortion in the helium cluster (Initial shape of the

He cluster: Distorted hexagonal bipyramidal and one helium atom holds the centre of the hexagonal plane) (Figure 2). Mainly the hexagonal He–plane gets distorted first and after that throughout the helium cluster distortion takes place and finally at 500 fs we observe the helium cluster without any specific geometry (Figure 3). In the case of the 225 K simulation we observe a maximum in the total energy profile at 160 fs because at that time step the geometry of the He cluster becomes distorted and a slight movement in three He atoms is observed towards the cage wall. Up to 310 fs the helium cluster remains inside the water cage only distortion from the previous arrangement took place but after that one of the He atoms among the previously mentioned three He atoms, started to move towards one of the hexagonal faces of the H<sub>2</sub>O cage (Figure 3), at 395 fs the He atom is observed at the centre of the hexagonal face of the H<sub>2</sub>O cage and due to that a maximum at that time in the total energy profile is observed. After that energy decreases as the helium atom moves out of the cage (Figure 3). In the case of the 298 K simulation we see a maximum at 165 fs in the total energy profile due to slight change in orientation in the H-bonded H<sub>2</sub>O molecule of the water cage with the change in the geometry of the encapsulated He cluster (Figure 3). It is observed that some of the He atoms are gravitated towards the hexagonal faces of the water cage. As the time proceeds the total energy of the system decreases up to 330 fs and it is observed that the geometry of the water cage is less distorted respect to the geometry at the 165 fs. After that up to 500 fs, all the helium atoms stay inside the cage but the water cage gets distorted (Figure 3).

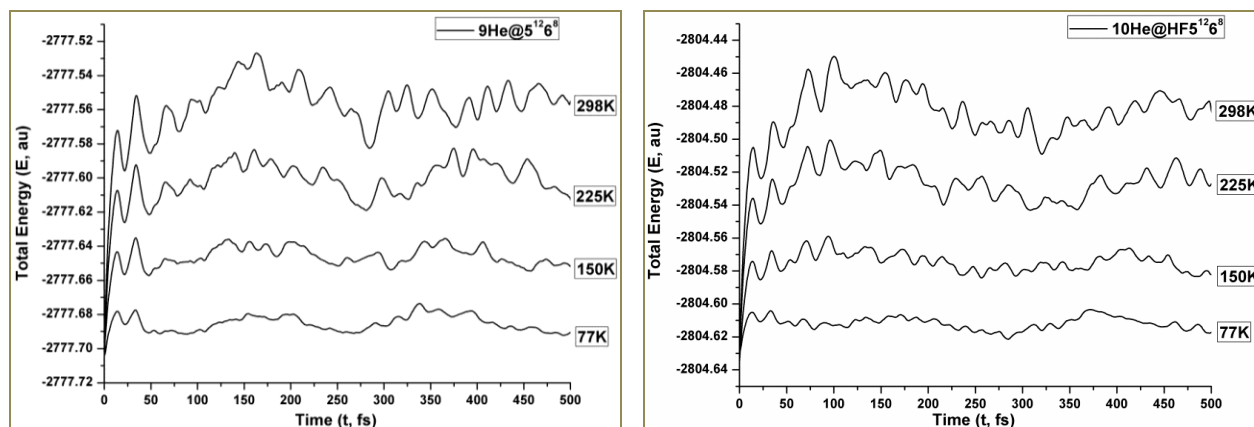


**Figure 2:** Variation of total energy for  $9\text{He}@5^{12}_6^8$  and  $10\text{He}@HF5^{12}_6^8$  at different temperatures.

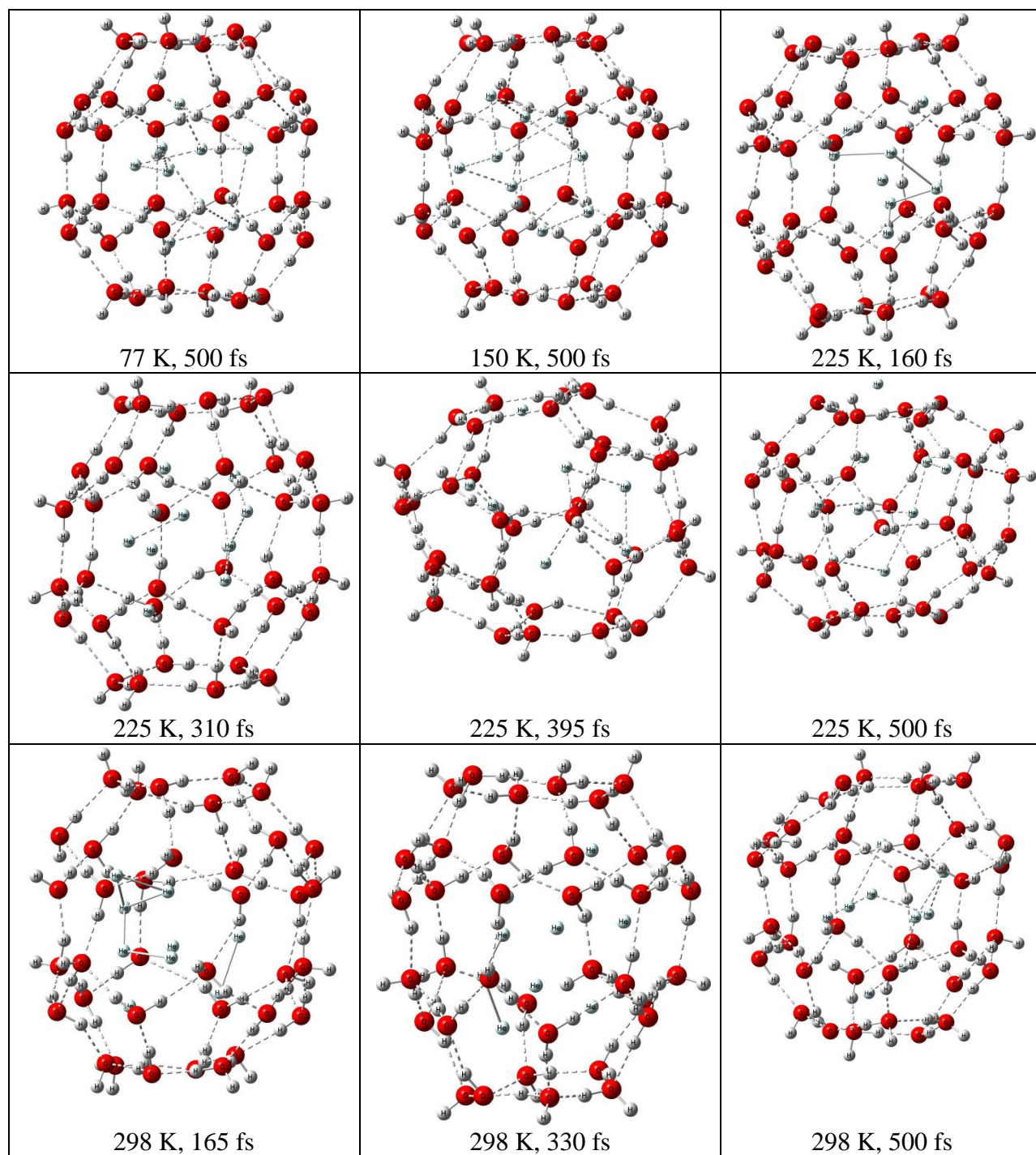


**Figure 3:** The structure of  $9\text{He}@5^{12}6^8$  at different time steps during the 500 fs simulation at different temperatures.

In the case of the  $10\text{He}@HF5^{12}6^8$  system, in the total energy profile crest and trough are observed presumably due to the molecular vibration ( $\text{H}_2\text{O}$ ), distortion in cage wall as well as due to the rearrangement of the He cluster (Figure 2). At 77 K and 150 K simulations no changes in the cage wall of the HF doped hydrate are observed but only certain change is observed in the

geometry of the encapsulated helium cluster. In the case of the 225 K simulation we observe a maximum at 95 fs, due to slight distortion in the water cage as well as the encapsulated He cluster losses its geometrical integrity and some of the He atoms moved towards the adjacent hexagonal faces (Figure 4). After that slight oscillation in the total energy profile is observed due to change in orientation of the H-bonded water molecules of the water cage but all the encapsulated He atoms stay in the water cage up to 500 fs. The total energy profile of the 298 K simulation shows a maximum at ~100 fs which accounts for the formation of a slightly distorted hexagonal face containing the HF unit in the water cage and the loss of geometrical shape of the encapsulated He cluster. It is observed that one of the He atoms moves towards one of the hexagonal faces of the cage (Figure 4). But no helium atom gets out of the cage up to 500 fs (Figure 4).

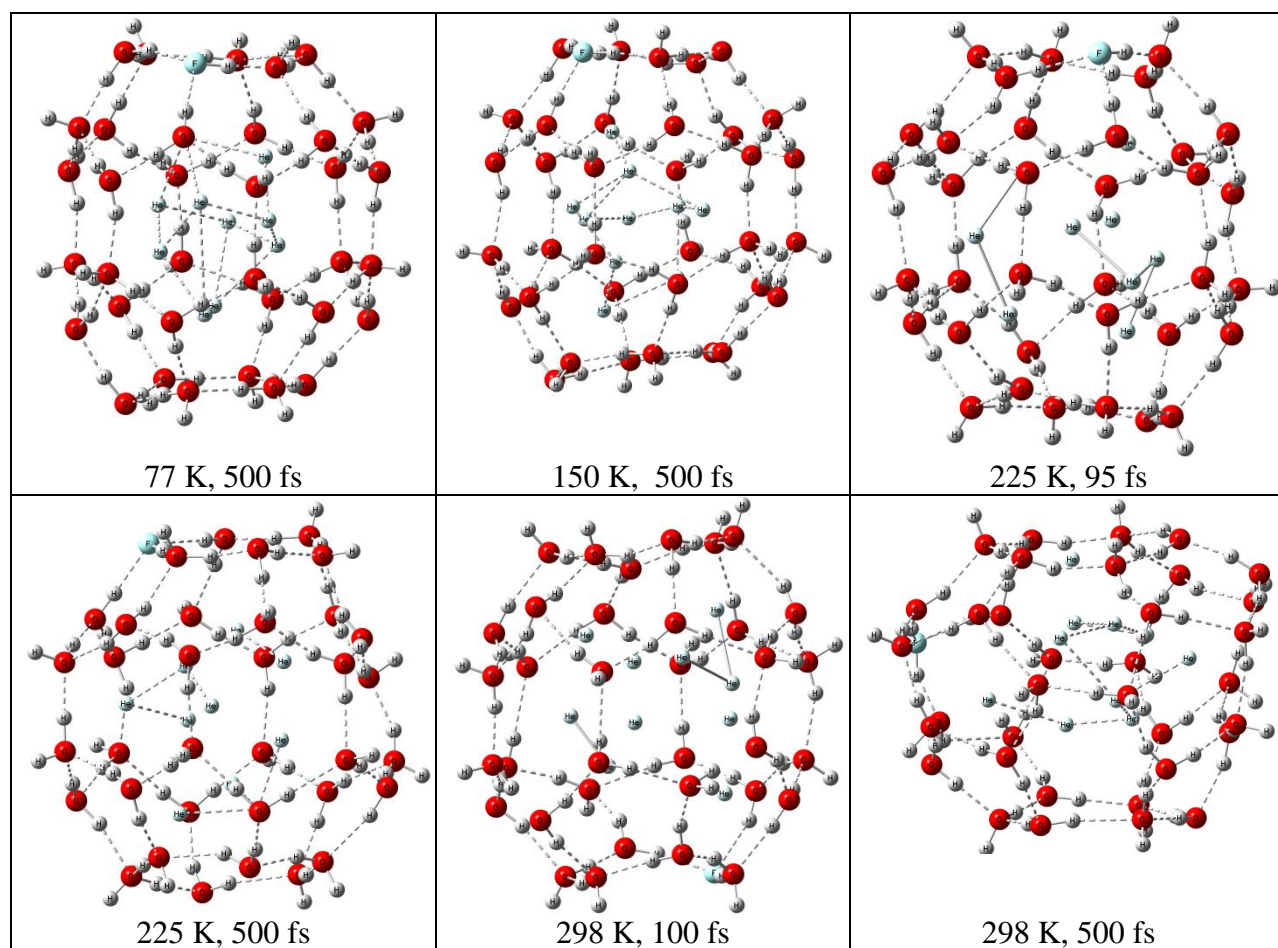
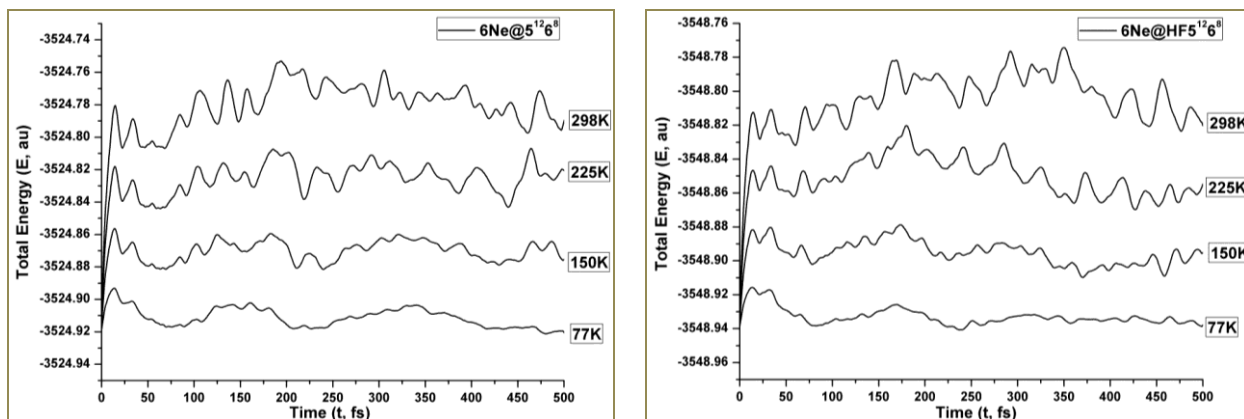


**Figure 4:** The structure of  $10\text{He}@\text{HF}_5^{12-6^8}$  at different time steps during the 500 fs simulation at different temperatures.

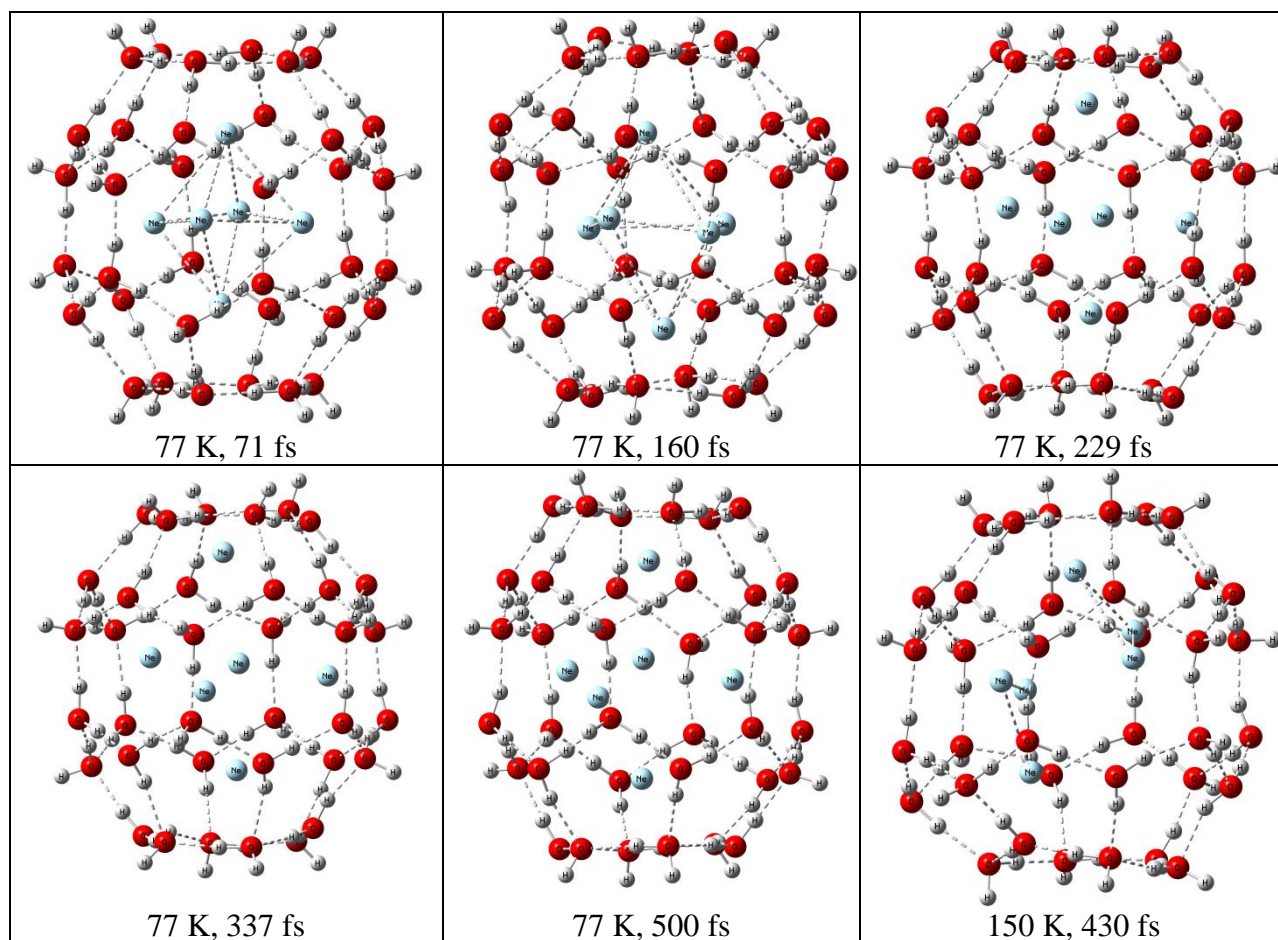
Thus we can conclude that  $9\text{He}@5^{12}\text{O}_6$  is kinetically stable at  $< 150$  K temperature whereas  $8\text{He}@5^{12}\text{O}_6$  may be kinetically stable up to 225 K.  $10\text{He}@HF5^{12}\text{O}_6$  is kinetically stable at  $< 225$  K temperature.

#### **$6\text{Ne}@5^{12}\text{O}_6$ & $6\text{Ne}@HF5^{12}\text{O}_6$ systems:**

Simulation of  $6\text{Ne}@5^{12}\text{O}_6$  system at 77 K reveals that  $5^{12}\text{O}_6$  cage can encapsulate up to 6 neon atoms. At 71 fs a broad minimum in the total energy profile is noticed which explains that the octahedral Ne cluster gets somewhat distorted at this time (Figure 5). At 160 fs two axial neon atoms of the Ne-octahedra slowly move towards the hexagonal face and one of the equatorial Ne atoms also moves towards the adjacent hexagonal faces of the water cage (Figure 6) and thus we see a maximum in the total energy plot at that time. At 229 fs a minimum in the total energy profile is observed which may be due to a little change in orientation (distortion of the cage) of the  $\text{H}_2\text{O}$  molecules in the cage (Figure 6). At 337 fs the cage gets distorted the most and two Ne atoms (one axial and one equatorial) move towards the adjacent face of the cage (hexagonal) (Figure 6). After that the energy of the system decreases and the rearrangement of the octahedral Ne-cluster starts as well as the two Ne atoms move again to the centre of the cage from the hexagonal face (Figure 6). The results of 150 K simulation of  $6\text{Ne}@5^{12}\text{O}_6$  system is almost similar to that in the 77 K simulation, excluding the fact that after 430 fs no reformation of the octahedral Ne cluster is seen but two individual triangular Ne-clusters form (due to that total energy of the system increases) and at 500 fs the triangular Ne-clusters (Figure 6) are formed. In the case of the 225 K simulation the molecular dynamics and the energetics are almost similar to those in the 150 K and 77 K cases, the differences are observed after 328 fs, when 3 Ne atoms start to form a triangular arrangement among the 6 Ne atoms inside the water cage, whereas remaining three stay individually without maintaining any geometry (Figure 6). Due to this a maximum in the total energy profile after 328 fs is seen and at 464 fs the energy of the system becomes maximum (Figure 5). 298 K simulation shows that the dynamics of the cage and the encapsulated Ne cluster are similar to that of the lower temperature simulations but after 300 fs the cage wall starts to distort and at 464 fs as well as at 500 fs three membered and four membered small water clusters in the cage wall are formed and the  $5^{12}\text{O}_6$  cage loses its integrity (Figure 6).



**Figure 5:** Variation of total energy for 6Ne@5<sup>12</sup>6<sup>8</sup> and 6Ne@HF5<sup>12</sup>6<sup>8</sup> at different temperatures.



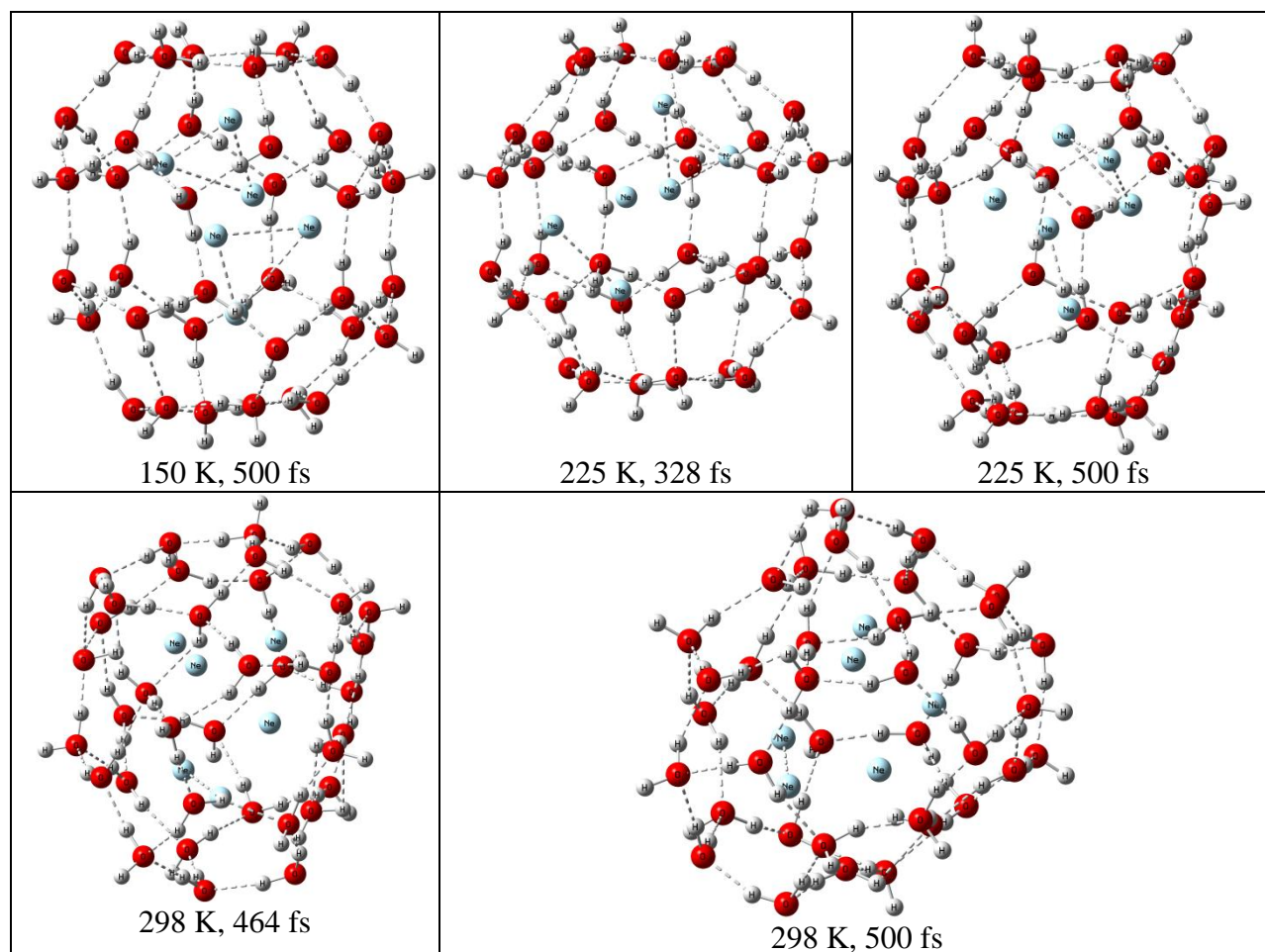


**Figure 6:** The structure of  $6\text{Ne}@5^{12}_6^8$  at different time steps during the 500 fs simulation at different temperatures.

The dynamics and energetics of the Ne-cluster inside the  $\text{HF}5^{12}_6^8$  cage at different temperatures are similar to that of the HF undoped case (Figure 5). Simulations at 77 K and 150 K temperatures reveal that the dynamics are similar to that of HF undoped cases, only exception is that the cage wall is somewhat distorted at all the sites other than the HF doped sites (Figure 7). In the case of the 225 K simulation the HF doped cage starts to get distorted from 150 fs onwards, and at 175 fs three membered and four membered water clusters are about to form in the cage wall (Figure 7). After that energy of the system decreases and three membered and four membered water clusters in the cage wall are formed. In the case of the 298 K simulation of the  $6\text{Ne}@5^{12}_6^8$  system it is observed that at 350 fs the HF doped cage distorts substantially and

the five membered and six membered faces of the cage wall form small three member and four membered clusters, the maximum in the energy profile at that time indicates that (Figure 5).

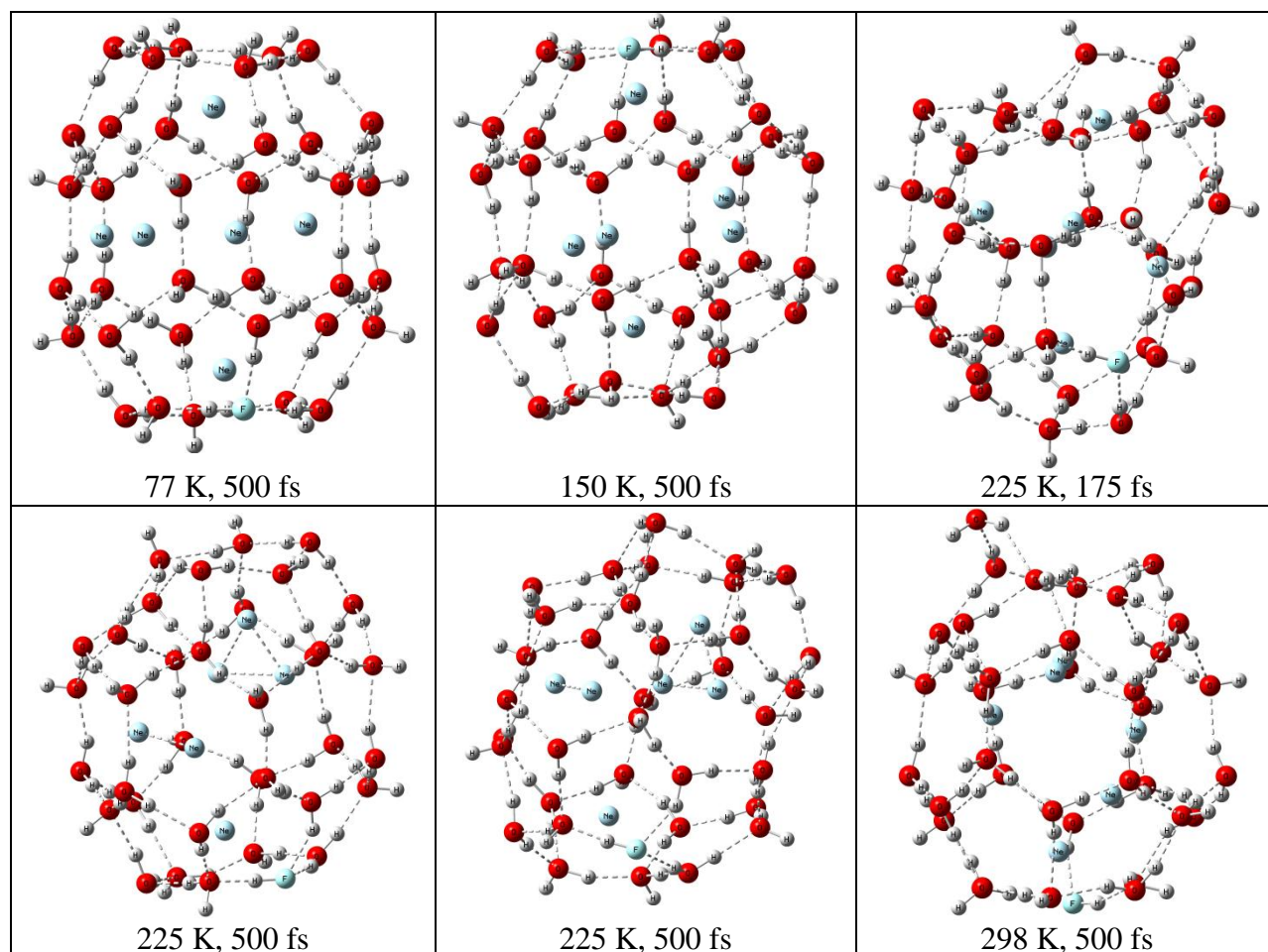


**Figure 7:** The structure of  $6\text{Ne}@HF5^{12}_6^8$  at different time steps during the 500 fs simulation at different temperatures.

From above discussion we can infer that  $6\text{Ne}@5^{12}_6^8$  and  $6\text{Ne}@HF5^{12}_6^8$  systems are kinetically stable at  $< 225$  K and  $< 150$  K temperatures respectively.

### $6\text{Ar}@5^{12}_6^8$ & $6\text{Ar}@HF5^{12}_6^8$ systems:

In the case of  $6\text{Ar}@5^{12}_6^8$ , during the entire 77 K simulation (500 fs) only molecular vibration (of the  $\text{H}_2\text{O}$  molecule) and rotation of Ng atoms are observed. In the case of the 150 K simulation at 140 fs and at 315 fs in both the cases the octahedral arrangement of the six Ar atoms gets disturbed (becomes distorted octahedron) and the total energy of the system increases at those two points (Figure 8). In the case of 225 K simulation at 115 fs and at 158 fs the energy of the

system increases due to the change in the geometry of the encapsulated Ar cluster (the octahedral shape is slightly distorted (Figure 9)). After that one of the Ar atoms moves towards a hexagonal face of the water cage and the octahedral Ar-cluster becomes more distorted and thereby energy of the system increases (at 363 fs, 428 fs and 456 fs) (Figure 8 & 10). At 298 K simulation, cage distortion starts from 101 fs and the Ar-cluster also gets slightly distorted. At 275 fs a maximum in the total energy profile is observed which accounts for the fact that the octahedral Ar-cluster gets distorted and its axial Ar atoms get compressed whereas the equatorial two Ar atoms move towards two adjacent hexagonal faces of the water cage. At 412 fs only one Ar atom moves to the centre of the approached hexagonal face of the cage and the cage distortion takes place as well from that hexagonal face. At 467 fs the Ar atom stays a little above the ruptured hexagonal face and cage is ruptured (Figure 9). In the case of the  $6\text{Ar}@HF5^{12}6^8$  system no structural change occurs for the 77 K and 150 K simulation during the 500 fs simulation time. But for the cases of 225 K and 298 K simulations it is observed that at  $\sim 175$  fs and at  $\sim 410$  fs there are maxima in the total energy profile (Figure 8). At  $\sim 175$  fs in both the cases the octahedral Ar-cluster gets distorted whereas at  $\sim 410$  fs one of the equatorial Ar atoms moves towards one of the hexagonal faces of the cage. But the distortion in Ar cluster and the deconstruction of the HF doped clathrate hydrate is more in the case of the 298 K simulation. Even we noticed the formation of triangular and square shaped  $\text{H}_2\text{O}$  clusters in the cage wall of HF doped clathrate (Figure). Deformation of the cage wall continues up to the end of the simulation. No cage rupture is observed in the site where HF is doped. Thus we should mention here that  $6\text{Ar}@5^{12}6^8$  and  $6\text{Ar}@HF5^{12}6^8$  both the systems are kinetically stable at  $< 225$  K temperature.

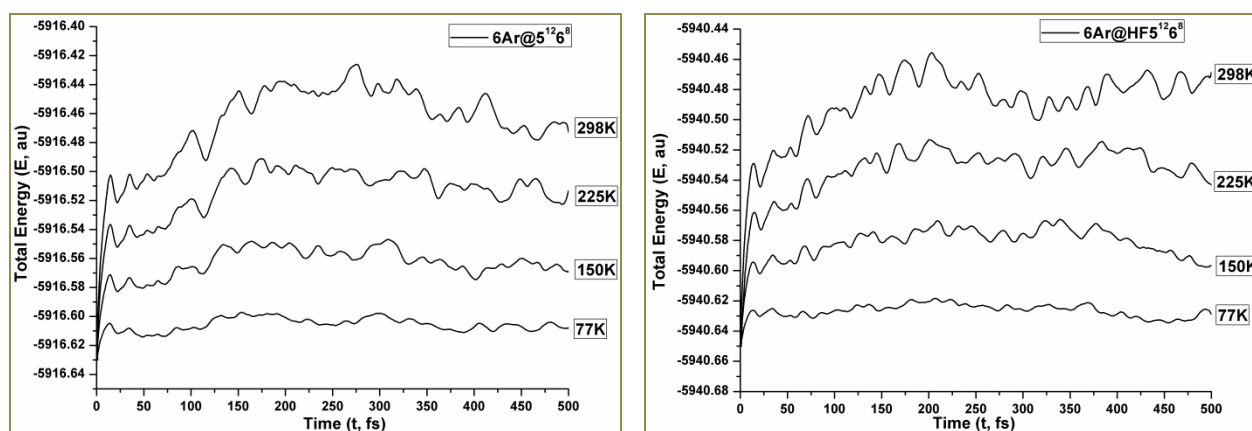


**Figure 8:** Variation of total energy for  $6\text{Ar}@5^{12}6^8$  and  $6\text{Ar}@HF5^{12}6^8$  at different temperatures.

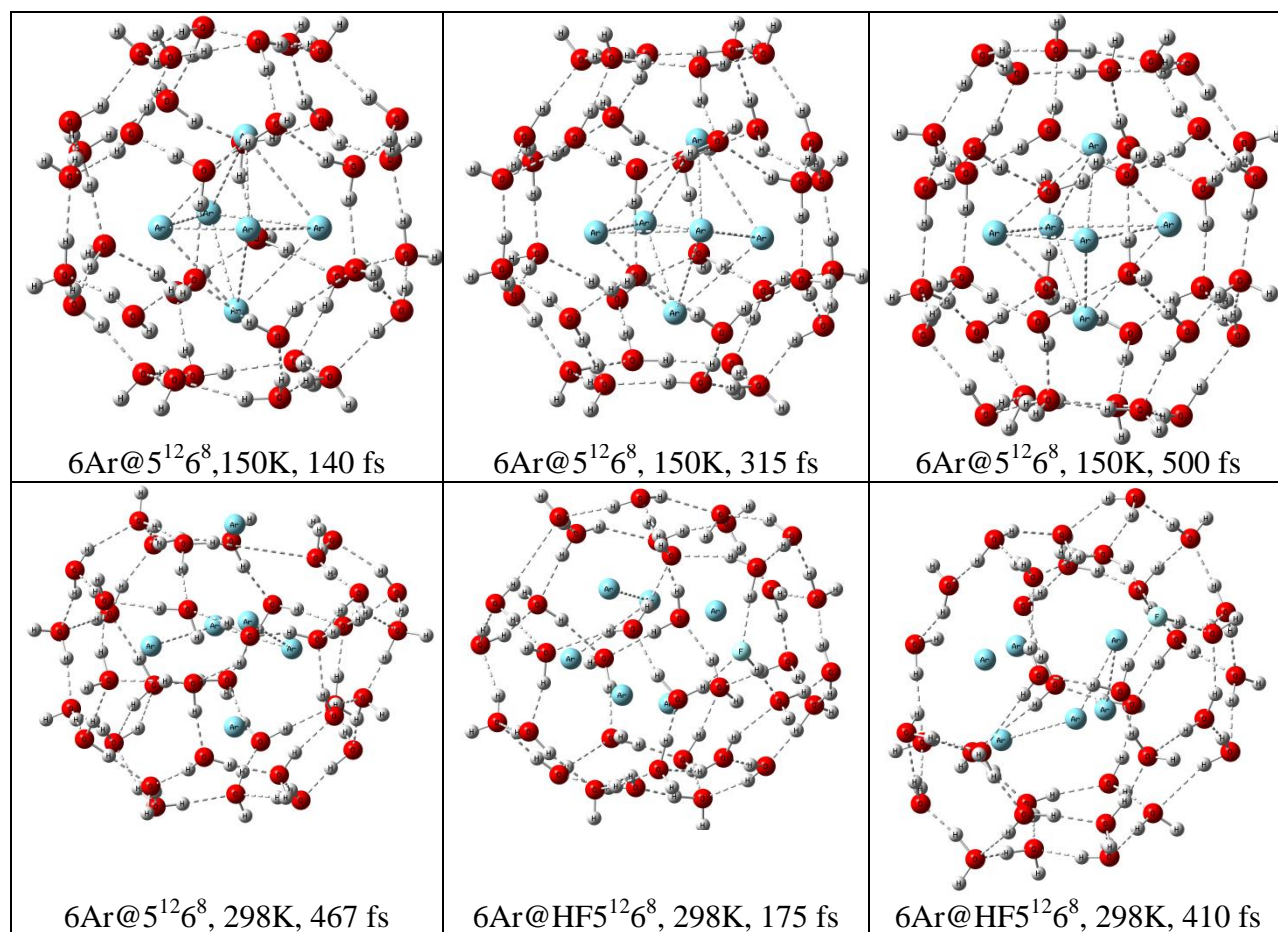


**Figure 9:** The structure of 6Ar@5<sup>12</sup>6<sup>8</sup> and 6Ar@HF5<sup>12</sup>6<sup>8</sup> at different time steps during the 500 fs simulation at different temperatures.

## Conclusion

The 5<sup>12</sup> clathrate hydrate and its HF doped analogue can encapsulate up to five helium atoms, three neon atoms and two argon atoms, but the encapsulation of only one of the each (He, Ne and Ar) atom is thermodynamically favourable. 5<sup>12</sup>6<sup>8</sup> can encapsulate nine helium atoms and HF5<sup>12</sup>6<sup>8</sup> can encapsulate ten helium atoms. Both 5<sup>12</sup>6<sup>8</sup> and HF5<sup>12</sup>6<sup>8</sup> can engage up to six neon and six argon atoms. The HF doping facilitates the noble gas encapsulation when the noble gas guest atom is larger in size and when the cage size decreases as well as the number of encapsulated Ng atom decreases to one. Electron density analysis reveals that Ng---O, Ng---F, and Ng---Ng interactions are purely noncovalent in nature. 5<sup>12</sup> and HF5<sup>12</sup> cages can hold one helium, one neon or one argon atom up to 500 fs at 298 K. In the case of 5<sup>12</sup> cage, HF doping

increases the resistance towards any distortion in the cage wall. The  $5^{12}6^8$  cage can encapsulate 8 He atoms without any distortion in the  $5^{12}6^8$  cage up to 500 fs, at  $\leq 225$  K. The  $HF5^{12}6^8$  cage can hold up to 10 He atoms up to 500 fs at 298 K but there is distortion in the cage wall. Dynamics of  $6Ne@5^{12}6^8$  and  $6Ne@HF5^{12}6^8$  systems reveal that  $5^{12}6^8$  and  $HF5^{12}6^8$  cages can hold 6 Ne atoms up to 500 fs at  $\leq 225$  K and  $\leq 150$  K temperatures respectively.  $5^{12}6^8$  and  $HF5^{12}6^8$  cages can hold 6 Ar atoms up to 500 fs at  $\leq 225$  K temperature. At 298 K temperature both the cage walls of  $6Ar@5^{12}6^8$  and  $6Ar@HF5^{12}6^8$  are ruptured and formation of small four membered and three membered water clusters are observed in the cage wall. Cage distortion and rupture in the above mentioned systems arise after a certain temperature due to their kinetic instability though they are thermodynamically stable. Thus AIMD study reveals that noble gas encapsulated  $5^{12}$ ,  $HF5^{12}$  and  $5^{12}6^8$ ,  $HF5^{12}6^8$  systems are kinetically stable as well but up to certain temperatures.

### Acknowledgments

SM thanks UGC, New Delhi for financial assistance. P.K.C. would like to thank the DST, New Delhi, for the J.C. Bose National Fellowship.

### References

- 1) (a) L. Rayleigh, W. Ramsay, *Proc. R. Soc. London*, 1894–1895, **57** (1), 265.  
(b) L. Rayleigh, W. Ramsay, *Philos. Trans. R. Soc. London, Ser. A*, 1895, **186**, 187.
- 2) P. Villard, *C. r. hebd. Seanc. Acad. Sci., Paris*, 1896, **123**, 377.
- 3) R. de Forcrand, *C. r. hebd. Seanc. Acad. Sci., Paris*, 1923, **176**, 355.
- 4) R. de Forcrand, *C. r. hebd. Seanc. Acad. Sci., Paris*, 1923, **181**, 15.
- 5) D. Londono, W. F. Kuhs, and J. L. Finney, *Nature*, 1988, **332**, 141.
- 6) R. V. Belosludov, Y. Kawazoe, E.V. Grachev, Yu A. Dyadin, V. R. Belosludov, *Solid State Commun.*, 1999, **109**, 157.
- 7) G. P. Arnold, R. G. Wenzel, S. W. Rabideau, N. G. Nereson, and A. L. Bowman, *J. Chem. Phys.*, 1971, **55**, 589.
- 8) Y. A. Dyadin, E. G. Larionov, A. Yu. Manakov, F. V. Zhurko, E. Ya. Aladko, T. V. Mikina and V. Yu. Komarov, *Mendeleev Commun.*, 1999, **9**(5), 209.

- 9) L. Hakim, K. Koga, H. Tanaka, *Physica A*, 2010, **389**, 1834.
- 10) A.Y. Dyadin, E.G. Larionov, E.Y. Aladko, A.Y. Manakov, F.V. Zhurko, T.V. Mikina, V.Y. Komarov, E.V. Grachev, *J. Struct. Chem.*, 2000, **40**, 790.
- 11) Y. A. Dyadin, E. G. Larionov, D. S. Mirinski, T. V. Mikina and L. I. Starostina, *Mendeleev Commun.*, 1997, **7**(1), 32.
- 12) J. A. Abbondondola, E. B. Fleischer, K. C. Janda, *J. Phys. Chem. C.*, 2009, **113**, 4717.
- 13) J. A. Abbondondola, E. B. Fleischer, K. C. Janda, *AIChE Journal*, 2010, **56**, No. 10.
- 14) B. J. Anderson, *Fluid Phase Equilib.*, 2007, **254**, 144.
- 15) W. F. Clausen, *J. Chem. Phys.*, 1951, **19**, 259.
- 16) W. F. Clausen, *J. Chem. Phys.*, 1951, **19**, 1425.
- 17) H. R. Muller, v. M. Stackelberg, *Naturwissenschaften*, 1952, **39**, 20.
- 18) E. D. Sloan, *Clathrate Hydrates of Natural Gases*; Marcel Dekker Inc.: New York, 1998.
- 19) S. Mondal, S. Ghosh, P. K. Chattaraj, *J. Mol. Model.*, 2013, **19**, 2785.
- 20) P. K. Chattaraj, S. Bandaru and S. Mondal, *J. Phys. Chem. A*, 2011, **115**, 187.
- 21) S. Mondal, S. Giri, and P. K. Chattaraj, *J. Phys. Chem. C*, 2013, **117**, 11625.
- 22) S. Mondal, S. Giri, and P. K. Chattaraj, *Chem. Phys. Lett.*, 2013, **578**, 110.
- 23) D. Marx, J. Hutter, In *Proceedings of Modern Methods and Algorithms of Quantum Chemistry*, Julich, E. Grotendorst, Ed., John von Neumann Institute for Computing: Jurich, Germany, 2000.
- 24) H.B. Schlegel, J.M. Millam, S.S. Iyengar, G.A. Voth, A.D. Daniels, G.E. Scuseria, M.J. Frisch, *J. Chem. Phys.*, 2011, **114**, 9758.
- 25) S.S. Iyengar, H.B. Schlegel, J.M. Millam, G.A. Voth, G.E. Scuseria, M.J. Frisch, *J. Chem. Phys.*, 2011, **115**, 10291.
- 26) H.B. Schlegel, S.S. Iyengar, X. Li, J.M. Millam, G.A. Voth,; G.E. Scuseria, M.J. Frisch, *J. Chem. Phys.*, 2002, **117**, 8694.
- 27) R. G. Pearson, *J. Chem. Edu.*, 1987, **64**, 561.
- 28) R. G. Parr, P. K. Chattaraj, *J. Am. Chem. Soc.*, 1991, **113**, 1854.
- 29) P. W. Ayers, R. G. Parr, *J. Am. Chem. Soc.*, 2000, **122**, 2010.
- 30) S. Pan, M. Solà, and P. K. Chattaraj, *J. Phys. Chem. A*, 2013, **117**, 1843.

- 31) (a) E. Chamorro, P. K. Chattaraj, P. Fuentealba, *J. Phys. Chem. A*, 2003, **107**, 7068. (b) R. Parthasarathi, M. Elango, V. Subramanian, P. K. Chattaraj, *Theo. Chem. Acc.*, 2005, **113**, 257.
- 32) P. Geerlings, F. De Proft, W. Langenaeker, *Chem. Rev.*, 2003, **103**, 1793.
- 33) R. G. Parr, R. A. Donnelly, M. Levy, W. E. Palke, *J. Chem. Phys.*, 1978, **68**, 3801.
- 34) P. K. Chattaraj, U. Sarkar, D. R. Roy, *Chem. Rev.*, 2006, **106**, 2065.
- 35) P. K. Chattaraj, D. R. Roy, *Chem. Rev.*, 2007, **107**, PR46-PR74.
- 36) R. G. Parr, L. v. Szentpaly, S. Liu, *J. Am. Chem. Soc.*, 1999, **121**, 1922.
- 37) T. A. Koopmans, *Physica.*, 1933, **1**, 104.
- 38) J. F. Janak, *Phys. Rev. B.*, 1978, **18**, 7165.
- 39) GaussView, Version 5, R. Dennington, T. Keith, J. Millam, *Semichem Inc.* Shawnee Mission KS. 2009.
- 40) M. J. Frisch et al., Gaussian09, Revision A.1, Gaussian, Inc.: Pittsburgh, PA, 2009.
- 41) J. D. Chai, M. Head-Gordon, *Phys. Chem. Chem. Phys.*, 2008, **10**, 6615.
- 42) S.F. Boys, F. Bernardi, *Mol. Phys.*, 1970, **19**, 553.
- 43) A. D. Becke, *J. Chem. Phys.*, 1993, **98**, 5648.
- 44) C. Lee, W. Yang, R. G. Parr, *Phys. Rev. B*, 1988, **37**, 785.
- 45) M. Ceppatelli, R. Bini and V. Schettino, *Phys. Chem. Chem. Phys.*, 2011, **13**, 1264.
- 46) T. Lu, F. W. Chen, *J. Comput. Chem.*, 2012, **33**, 580.
- 47) R. F. W. Bader, P. J. MacDougall, and C. D. H. Lau, *J. Am. Chem. Soc.*, 1984, **106**, 1594.
- 48) R. F. W. Bader, *Atoms in Molecules: A Quantum Theory*, Clarendon press, Oxford, UK, 1990.
- 49) M. Khatua, S. Pan and P. K. Chattaraj, *J. Chem. Phys.*, 2014, **140**, 164306.
- 50) D. Cremer, E. Kraka, *Angew. Chem. Int. Edt.*, 1984, **23**, 627.
- 51) M. Ziolkowski, S. J. Grabowski, J. Leszczynski, *J. Phys. Chem. A*, 2006, **110**, 6514.